Int. J. Heat Mass Transfer. Vol. 34, No. 10, pp. 2669–2673, 1991
Printed in Great Britain

0017–9310/91 $3.00+0.00

Vaporization behavior of fuel droplets in a hot air stream

S. K. AGGARWAL and G. CHEN
Department of Mechanical Engineering, University of Illinois at Chicago,
P.O. Box 4348, Chicago, IL 60680, U.S.A.

and

T. A. JACKSON and G. L. SWITZER
Wright Patterson AFB, OH 45433, U.S.A.

(*Received* 24 *January* 1990 *and in final form* 14 *November* 1990)

1. INTRODUCTION

THE GASIFICATION behavior of a liquid droplet provides a fundamental input for the modeling of many spray systems, and has been studied extensively [1–4]. Theoretical analysis for the multicomponent fuel droplet presents several complexities absent in a similar analysis for the single component droplet. First, the phase-change process at the droplet surface and the transport of a fuel vapor mixture in the gas phase need to be properly described. Second, the evaporation process is inherently time varying due to the continuous change in the composition and temperature of the droplet as vaporization proceeds. Another difference between the two cases is due to the phenomenon of microexplosion [2].

The earlier viewpoint [2] of multicomponent droplet vaporization assumes that the composition and temperature within the droplet are spatially uniform but time varying. Such theories predict that the gasification process is similar to batch distillation in that the sequence of gasification is controlled by the volatility differentials among the different components. However, Sirignano [4] showed that even in the limit of high vortex strength, the internal liquid circulation can only reduce the characteristic length scale for diffusion by a factor of three. Landis and Mills [5] investigated the vaporization of a bi-component fuel droplet in a stagnant atmosphere. A quasi-steady gas-phase model was used and the equations governing the unsteady mass and heat diffusion within the droplet were solved numerically. Results when compared with rapid mixing behavior showed significant differences. A unique feature of the diffusion-dominated droplet gasification mechanism is the possible attainment of approximately steady-state temperature and concentration profiles within the droplet, which then leads to a steady-state gasification rate. Based on this concept, Law and Law [6] formulated a d^2-law model for multicomponent droplet vaporization and combustion.

As indicated above, the literature on the gasification behavior of an isolated droplet is extensive. However, most of these studies deal with droplet combustion or evaporation under high-temperature conditions. Not much information is available on the behavior of evaporating droplets in relatively low-temperature air streams. Under such conditions, the possibility of an envelope flame is precluded and the droplet gasification rate is low. The droplet heat-up time may not be negligibly small compared to its lifetime, although the latter is relatively large and the liquid-phase transient processes may still be important.

In this paper, the vaporization behavior of pure and multicomponent fuel droplets flowing in a well-characterized laminar flow is studied. The predictions of three vaporization models are compared with the experimental data.

2. THEORETICAL MODEL

The theoretical model involves the calculation of velocity, size, and surface properties of an evaporating droplet along its trajectory in a laminar hot air flow. The time-dependent Lagrangian equations for the droplet position, velocity, and size are solved numerically.

In most circumstances, the gas-phase transient time is much smaller than the characteristic time for the liquid-phase processes. Consequently, the gas-phase processes can be considered as quasi-steady and the equations can be solved analytically [3] for the non-dimensional mass evaporation rate $\dot{m}$, the fractional mass evaporation rate ε_i, and the effective latent heat $\hat{H}$ as

$$\dot{m} = \ln\left(1+\frac{Y_{fs}-Y_{f\infty}}{1-Y_{fs}}\right) \tag{1}$$

$$\varepsilon_i = \frac{\dot{m}_i}{\dot{m}} = Y_{is}+(1-Y_{fs})\frac{Y_{fis}-Y_{fi\infty}}{Y_{fs}-Y_{f\infty}} \tag{2}$$

$$\hat{H} = \frac{(1-Y_{fs})(\hat{T}_\infty-\hat{T}_s)}{Y_{fs}-Y_{f\infty}}. \tag{3}$$

At any given time instant, the gas-phase species mole fraction at the droplet surface can be obtained by means of Raoult's law

$$X_{is} = X_{fl}X_{oi} \tag{4}$$

where X_{oi} is the equilibrium vapor mole fraction for the pure liquid i given by the Clausius–Clapeyron relation

$$X_{oi} = (1/P)\exp\{L_iW_i/R[(T_{ib})^{-1}-(T_s)^{-1}]\}. \tag{5}$$

Finally, X_{is} is related to the gas-phase species mass fraction, Y_{is}, through

$$Y_{is} = X_{is}W_i\Big/\left\{\left(1-\sum_{i=1}^{n}X_{is}\right)+\sum_{i=1}^{n}X_{is}W_i\right\} \tag{6}$$

where W_i is the ratio of the molecular weight of the ith vaporizing species to an average molecular weight of all the non-condensable inert species at the droplet surface. As indicated above, the liquid-phase transient processes appear through the variables X_{fl} and T_s. To examine their influence, three liquid-phase models considered are the infinite-diffusion, diffusion-limit and thin-skin models. The first two models have been described elsewhere [7, 8]. The implicit assumption in the infinite-diffusion model is that the internal circulation is so fast that the droplet temperature and composition are maintained spatially uniform, though still temporally varying. The volatile components are continuously brought to the droplet surface where they are preferentially vaporized. The temporal variations of droplet composition and temperature are determined from the overall mass and energy conservation equations [8]. In the diffusion-limit model, the transient heat and mass transport in the liquid are assumed to be governed by the unsteady heat and mass diffusion equations [7].

NOMENCLATURE

C_D drag coefficient
C_p specific heat at constant pressure
D mass diffusivity
g gravitational acceleration
h enthalpy
H effective latent heat
$\hat{H}$ H/L_b
K $\rho D/\alpha_l\rho_l$
L latent heat
M mass
m mass gasification rate at surface
$\hat{m}$ $m/4\pi\rho D\tau_s$
n number of species
P pressure
r radial distance
$\bar{r}$ dimensional radial distance
R gas constant
Re Reynolds number
t time
$\bar{t}$ dimensional time
T temperature
$\hat{T}$ C_pT/L_b
$\bar{T}$ dimensional temperature
V velocity
W molecular weight
x gas phase mole fraction
X liquid mole fraction
Y mass fraction.

Greek symbols
α thermal diffusivity
ε fractional mass vaporization rate
η $K\hat{m}\,Le(1-\bar{r})$
λ thermal conductivity
μ viscosity
ρ density.

Subscripts
b value corresponding to normal boiling temperature
f fuel
g gas phase
l liquid phase
r value corresponding to reference state
s droplet surface
∞ value at infinity.

The thin-skin model is based on the assumption of high liquid Lewis number and high droplet evaporation rate. Under these conditions, we may assume that the droplet surface temperature and its concentration distributions remain constant at T_s and $Y_{fl}(\hat{r})$, respectively. This is an extension of the single-component d^2-law to the multi-component case. With the above assumptions, it is unnecessary to study transient liquid-phase processes, the effective latent heat is equal to the actual latent heat, and the constant concentration profiles are given by

$$\frac{1}{\bar{r}^2}\frac{\mathrm{d}}{\mathrm{d}\bar{r}}\left(\bar{r}^2\frac{\mathrm{d}Y_{fl}}{\mathrm{d}\bar{r}}\right) = Le_l\,K\hat{m}\bar{r}\frac{\mathrm{d}Y_{fl}}{\mathrm{d}\bar{r}}. \tag{7}$$

The solution of equation (7) is

$$Y_{fl}(\bar{r}, T_s) = Y_{fl_0}\left\{1+\left[\frac{1/x_f}{\sum_{j=1}^{n} Y_{j_0}/x_j}-1\right]\exp\left[-K\hat{m}\,Le_l(1-\bar{r})\right]\right\}. \tag{8}$$

The only unknown parameter T_s can be found by solving equations (1)–(3).

As far as the convective correction is concerned, most approaches are semi-empirical. At higher Reynolds numbers, the Ranz–Marshall correlation [3] is frequently adopted. However, the comparison of calculated and experimental results indicated that the following relation [9] provides the best correlation in the present study:

$$\frac{\hat{m}_{cont}}{\hat{m}_s} = 1+0.24Re^{1/2}. \tag{9}$$

The relative gas velocity also produces a drag force. At any time t, the droplet trajectory can be found from the following equation:

$$\rho_l\pi r_s^3\frac{\mathrm{d}Z_d^2}{\mathrm{d}t^2} = \frac{3}{8}\pi r^2\rho_\infty\left|V_\infty-\frac{\mathrm{d}Z_d}{\mathrm{d}t}\right|\left(V_\infty-\frac{\mathrm{d}Z_d}{\mathrm{d}t}\right)C_D - g(\pi r^3)(\rho_l-\rho_\infty) \tag{10}$$

where C_D is the drag coefficient and is correlated to the Reynolds number [10] as

$$C_D = 27Re^{-0.84}. \tag{11}$$

The droplet equations for the instantaneous position, velocity, and size are solved by a second-order Runge–Kutta scheme with a variable time step.

The classical study of droplet vaporization and combustion assumes that the latent heat, the specific heat, the conductivity, and the product ρD are constants, and that the Lewis number $Le = (\lambda/C_p\rho D)$ in unity. In reality, these properties are strong functions of temperature and species concentrations. To consider these effects, a reference state scheme proposed by Law and Williams [11], which differs from the usual one-third rule, is used in the present study. Another important property is the latent heat L_i. In the present study, the ambient temperature is relatively low such that the droplet surface temperature is much lower than the boiling temperature. In such cases, it is incorrect to use constant L_i at the boiling temperature. Here, a modified Watson relation [8] is used to calculate L_i as a function of T_s.

3. RESULTS AND DISCUSSION

The results are obtained for three fuels, namely hexane, decane, and a mixture of hexane and decane. For each case, the predictions of three vaporization models are compared with the measurements. In the experimental facility, a droplet-on-demand generator was built to inject fuel droplets into a well-controlled laminar heated air flow in a square test section. The air velocity and temperature fields needed for the droplet calculations were obtained experimentally. The droplet velocity and size along its trajectory were measured using the Phase-Doppler Particle Analyzer. The details of the experiments are given in refs. [8, 12].

Figure 1 shows the predicted and experimental droplet velocities along its trajectory. The measured gas velocity is also shown. The droplet velocity, which is higher than the gas velocity at the injection point, relaxes rapidly to an equilibrium value and then follows the variation of gas velocity along the trajectory. The important observation is that the calculated values agree very well with the experimental data. This means that the solid sphere drag correlation works well for the present situation. However, the properties of the gas film surrounding the droplet need to be calculated accurately.

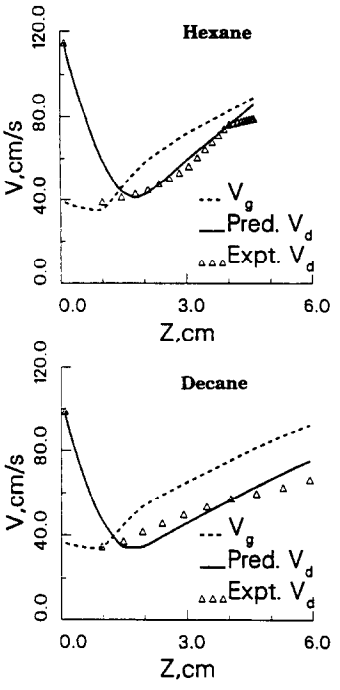

FIG. 1. Comparison of predicted and experimental droplet velocity along the trajectory.

Figure 2 shows the variation of the droplet diameter squared obtained experimentally and predicted by the thin-skin, diffusion-limit and infinite-diffusion models. Note that several data sets were obtained to assess the repeatability of data, although only one is shown. The overall agreement between predictions and experiments is quite good. For hexane, the calculated values are not very sensitive to the models. However, for decane, some sensitivity to the models is indicated, where the diffusion limit and infinite diffusion models show better agreement with the experimental data compared to the thin-skin model. These results can be explained by following the droplet surface temperature history. For hexane, the boiling temperature is relatively low, and the evaporation proceeds at a relatively fast rate. However, the latent heat needed for phase change is more than the heat transferred to the droplet surface. Consequently, the surface temperature would decrease until the heat needed for evaporation is provided by the ambiance. Therefore, the wet-bulb temperature is below the initial droplet temperature. The liquid-phase transient time is very short, and all three models predict almost the same surface temperature and, therefore, the droplet size variation is not sensitive to the models. For decane, however, the wet-bulb temperature is relatively high and the droplet transient heating becomes important. As a result, the vaporization behavior is sensitive to the models. Initially, the evaporation rate is very low and the amount of heat needed for evaporation is smaller than the heat transferred to the droplet surface. Consequently, the droplet temperature keeps increasing until it reaches an equilibrium temperature. Because the thin-skin model neglects the transient droplet heating, it predicts a faster vaporization rate than the other two models. Thus, the important observation is that the difference between the models is more significant for heavier fuels which have higher boiling temperatures and, thus, a longer transient heating period. It is also important to note that for the conditions considered the rate of heat transport to the surface is not much faster than the rate of heat transport within the droplet for the diffusion-limit model. Consequently, this model predicts almost the same vaporization rate as the infinite-diffusion model. However, for higher ambient temperatures, the rate of heat transfer to the droplet surface would be higher, and the difference between these two models will become apparent [8].

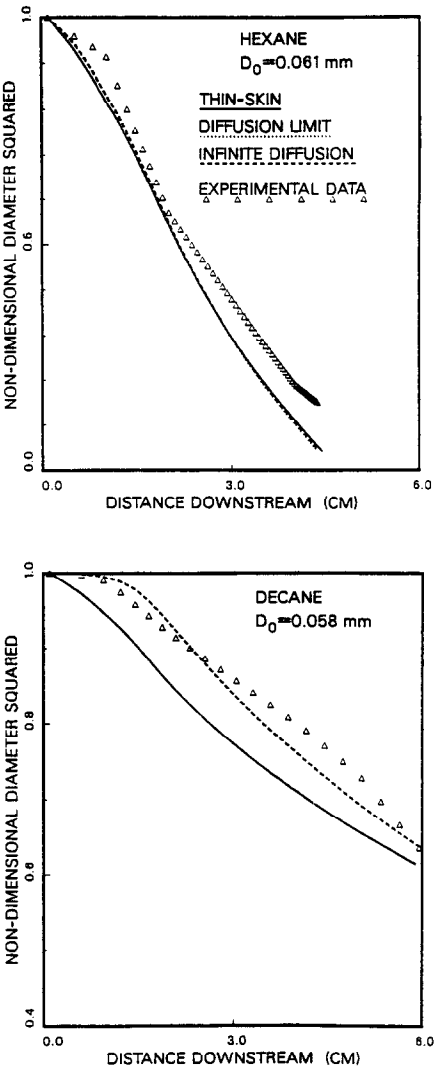

FIG. 2. Diameter squared along the trajectory of a fuel droplet.

Figure 3 shows the variation of the diameter squared along the trajectory of a hexane/decane droplet with the initial mass fraction of each being 0.5. It is interesting to note that the experimental data indicates a batch-distillation type of behavior, which is better simulated by the infinite-diffusion model. It means that the assumption of a spatially uniform liquid temperature and composition may be a good approximation for the present case. This is due to the slow rate of vaporization at relatively low environment temperature which makes the droplet evaporation time comparable to the thermal/mass diffusion times. The thin-skin model does not show as good an agreement as the other two models. This is due to the excessively slow rate of evaporation and long liquid transient time causing the assumption of constant temperature and composition profiles to deviate from the real situation.

Figure 4 shows the variation of the surface mass fraction of liquid hexane and the surface temperature along the droplet

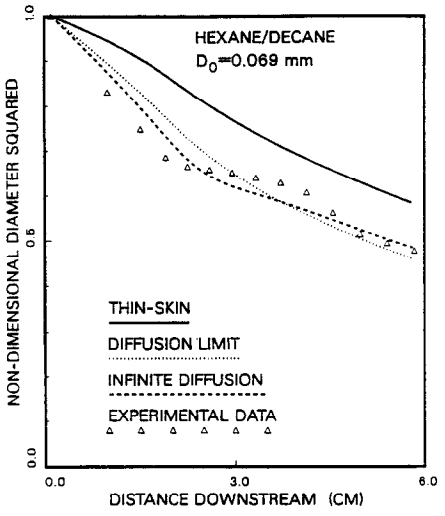

FIG. 3. Diameter squared along the trajectory for a multicomponent fuel droplet.

trajectory. Significant disagreements exist among the three models. For the thin-skin model, the surface concentration as well as temperature, by definition, have constant values. For the diffusion-limit model, the surface concentration initially decreases much faster than that for the infinite-diffusion model and then attains an almost constant value. For the latter model, the mass fraction of hexane decreases steadily due to the preferential vaporization of more volatile species, whereas the surface temperature initially has a constant value given by the wet-bulb temperature of the hexane component. It then continues to increase slowly as the wet-bulb temperature increases following the change in the liquid surface composition. Finally it approaches the wet-bulb temperature of decane. There is a transition region in between the two inflexion points of the curve which corresponds to the depletion of the hexane component.

The differences in the surface temperature and liquid concentrations cause differences in the predictions of surface vapor concentrations. It is observed, though not shown here, that the liquid concentration has a more dominant effect on the surface vapor concentration. As a result, the diffusion-limit model underpredicts the vaporization rate compared to the infinite-diffusion model. Note that this behavior is observed for low ambient temperatures. At relatively high ambient temperatures, the behavior is significantly different [3].

Figure 5 shows the sensitivity of predictions to the methods of calculating reference properties. For methods 1 and 2, the commonly-used one-third rule is employed. For method 3, the scheme of Law and Williams [11] is used to obtain the reference properties. An important observation is that method 1 which only considers the variable temperature effect shows significant differences with the experimental results. The difference between methods 2 and 3, which consider the temperature as well as fuel vapor effects, is negligible.

4. CONCLUSIONS

The vaporization behavior of pure and multicomponent fuel droplets in a laminar hot air flow has been studied. Predictions of three vaporization models have been compared with experimental data. Important conclusions are:

(1) The predicted droplet velocity shows excellent agreement with the measured data, indicating that the solid-sphere drag law is quite adequate for the conditions considered. However, an accurate calculation of the gas-film properties

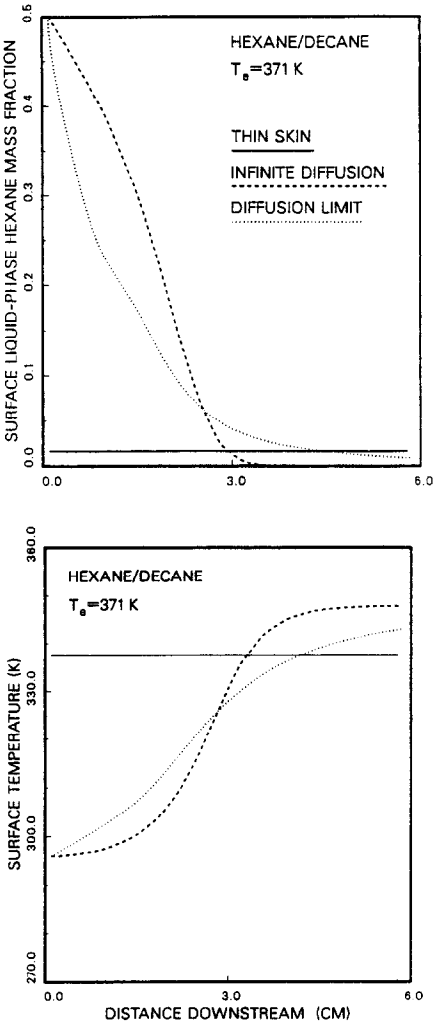

FIG. 4. Liquid hexane mass fraction and temperature at the droplet surface along the trajectory.

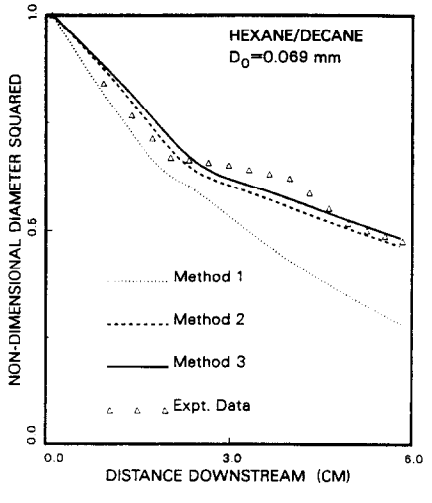

FIG. 5. Comparison of droplet size squared along the trajectory with different methods of calculating thermophysical properties.

has a strong effect on the predictions. The vaporization behavior of a hexane fuel droplet is not sensitive to the vaporization models. However, for less volatile fuels such as decane, the vaporization behavior shows some sensitivity to the models. The thin-skin model is not as accurate as the other two models which show excellent agreement with experimental data.

(2) The vaporization behavior of a multicomponent fuel droplet is better simulated by the infinite-diffusion model. However, the difference between the infinite-diffusion and diffusion-limit models is not very significant. The thin-skin model shows significant deviation from the experimental values.

(3) The variable property effects are important for an accurate prediction of droplet velocity and size. Not only the effect of temperature but also that of fuel vapor should be considered for calculating the thermophysical properties of the gas film surrounding the droplet. For low ambient temperatures, the accurate evaluation of the latent heat of fuel also has a noticeable effect on predictions.

To conclude, the present study illustrates that for relatively low ambient temperatures, both the infinite-diffusion and diffusion-limit methods can accurately predict the vaporization of pure as well as multicomponent fuel droplets. However, it is important to include the effects of variable thermophysical properties of the gas film outside the droplet as well as of the liquid-phase properties in a comprehensive manner. The present study also indicates the need for measuring the surface properties of a vaporizing multicomponent fuel droplet.

Acknowledgement—The financial support from the Air Force Office of Scientific Research is gratefully acknowledged.

REFERENCES

1. G. A. E. Godsave, Studies of the combustion of drops in a fuel spray—the burning of single drops of fuel, *Fourth Symposium (International) on Combustion*, p. 818. Williams and Wilkins, Baltimore (1953).
2. C. K. Law, Recent advances in droplet vaporization and combustion, *Prog. Energy Combust. Sci.* **8**, 169–199 (1982).
3. S. K. Aggarwal, A. Tong and W. A. Sirignano, A comparison of vaporization models in spray calculations, *AIAA J.* **22**, 1448–1457 (1984).
4. W. A. Sirignano, Theory of multicomponent fuel droplet vaporization, *Arch. Thermodyn. Combust.* **9**, 231–247 (1978).
5. R. B. Landis and A. F. Mills, Effect of internal diffusional resistance on the evaporation of binary droplets, Fifth Int. Heat Transfer Conf., Tokyo, Japan, Paper B7-9 (1974).
6. C. K. Law and H. K. Law, A d^2-law for multicomponent droplet vaporization and combustion, *AIAA J.* **20**, 522–527 (1982).
7. A. Y. Tong and W. A. Sirignano, Multicomponent droplet vaporization in a high temperature gas, *Combust. Flame* **66**, 221–235 (1986).
8. G. Chen, Vaporization behavior of pure and multicomponent fuel droplets in a hot air stream, M.S. Thesis, The University of Illinois at Chicago (1989).
9. G. A. Agoston, H. Wise and W. A. Rosser, Dynamic facts affecting the combustion of liquid spheres, *Sixth Symposium (International) on Combustion*, pp. 708–717. Reinhold, New York (1957).
10. R. A. Ingebo, Drag coefficients for droplets and solid spheres in clouds accelerating in air streams, NACA Technical Note 3762 (1956).
11. C. K. Law and F. A. Williams, Kinetics and convection in the combustion of alkane droplets, *Combust. Flame* **29**, 393–405 (1972).
12. T. A. Jackson, G. L. Switzer and S. K. Aggarwal, Measurements of droplet size and velocities in a laminar flow (under preparation).

Int. J. Heat Mass Transfer. Vol. 34, No. 10, pp. 2673–2676, 1991
Printed in Great Britain

0017–9310/91 $3.00 + 0.00

Calculation of scattering fractions for use in radiative flux models

R. KOENIGSDORFF, F. MILLER and R. ZIEGLER

Deutsche Forschungsanstalt für Luft- und Raumfahrt, Institut für Technische Thermodynamik, Pfaffenwaldring 38/40, 7000 Stuttgart 80, Germany

(*Received* 15 *August* 1990)

INTRODUCTION

ONE OF the most widely used methods to solve the equation of radiation transfer in participating media is the two-flux model. Apparently first introduced in the field of astrophysics where it is credited to Schuster and Schwarzchild [1], it has since been applied to problems in combustion, radiation transfer through insulation, solar energy absorption, atmospheric physics, and spectroscopy (where it is called Kubelka–Munk theory). The initial two-flux approximation, useful only for diffuse one-dimensional radiation transfer, has been extended to two and three dimensions—four and six fluxes respectively—and also has been modified to allow for partially collimated incident radiation. In the case of scattering media, factors that determine how the scattered light is distributed in the various axial directions appear in the flux equations. This note discusses and compares various methods of determining these scattering fractions for the two- and six-flux models starting from the properties of the scattering particles comprising the medium. Results are presented for two sample media, one purely scattering and one that also absorbs, and approximate methods for evaluating the scattering fractions are shown to be valid in certain ranges of the particle size parameter.

TWO-FLUX MODEL

The derivation of the two-flux equations has been rigorously laid out by Brewster [2] and others and will not be repeated in detail here. Briefly, however, the general equation of transfer for radiative intensity i' in a general direction S in a non-emitting participating medium [1]

$$\frac{\mathrm{d}i'_\lambda}{\mathrm{d}S} = -a_\lambda i'_\lambda(S) - \sigma_{s\lambda} i'_\lambda(S) + \frac{\sigma_{s\lambda}}{4\pi}\int_{4\pi} i'_\lambda(S,\omega_i)\Phi(\lambda,\omega,\omega_i)\,\mathrm{d}\omega_i \quad (1)$$

is simplified by assuming that the intensity is constant within each of two opposed solid angles (which are hemispheres in the two flux case) corresponding to two coordinate axis directions, say x and $-x$. This allows the integral in equation (1) to be solved for each hemisphere and results in the two equations